

December 1, 2022

Keywords or phrases:

Octet[®], COVID-19, SARS-CoV-2, Coronavirus, ACE2, Thermodynamics, Entropy, Enthalpy

Biophysical Characterization of the Binding of SARS-CoV-2 to the ACE2 Protein Using the Octet[®] R4 Bio-Layer Interferometry Platform

Nilshad Salim PhD, Bob Dass PhD, and David Apiyo PhD
Sartorius Corporation, 47661 Fremont Blvd, Fremont CA 94538 USA

Correspondence
Email: octet@sartorius.com

Introduction

Coronavirus disease 2019 (COVID-19) caused by the Severe Acute Respiratory Syndrome Corona Virus 2 (SARS-CoV-2) remains a global threat. Molecular level studies have been used to determine that the new virus SARS-CoV-2 like SARS-CoV binds to cells of respiratory mucosa through the angiotensin converting enzyme 2 (ACE2) receptors in the human body.¹ The structural analysis of SARS-CoV-2 has revealed that the virus consists of two types of molecules: RNA and proteins. The RNA encodes for 27 viral proteins, of which 16 are non-structural proteins (nsps), and 11 are accessory and structural proteins. There are 4 major structural proteins: nucleocapsid protein (N), spike surface glycoprotein (S), matrix protein (M), and small envelope protein (E).² The binding energy between the viral S protein and host ACE2 receptor is higher in the new virus versus SARS-CoV (-50.6 kcal/mol vs. -78.6 kcal/mol) suggesting a more stable complex,³ at the same time the affinity of the S protein of the SARS-CoV-2 for the ACE2 receptor is in the 15 nM range, which is about 10-20 times higher than SARS-CoV, an important factor for the differential infectivity.⁴

Find out more: www.sartorius.com/octet-BLI

Equilibrium stability and binding affinity parameters are often evaluated using different techniques; for example, molecular dynamics simulations can be used to estimate these parameters *in silico* while analytical instruments such as circular dichroism (CD) can be used in the lab for free energy evaluations and isothermal calorimetry systems for enthalpic and entropic thermodynamics parameters. In this application note, we deploy the use of the modular Octet® R4 BLI system to characterize the binding of SARS-CoV-2 to the various molecules at play (Figure 1) during infectivity (ACE2 protein, Spike protein-S, Receptor binding domain RBD and the trimeric SARS-CoV-2 S protein). This establishes the Octet® BLI system as an advanced platform that simplifies and accelerates workflows for the rapid evaluation of the thermodynamics at play during molecular interactions.

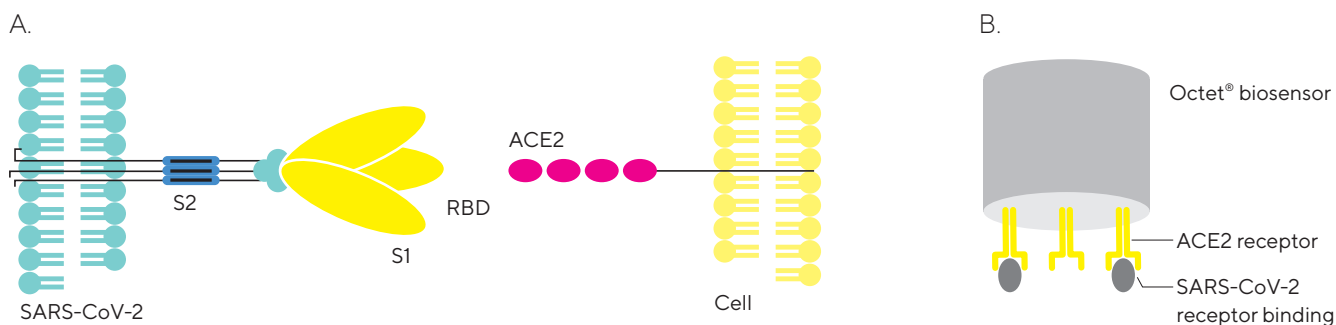


Figure 1: A Schematic of the Molecules at Play During SARS-CoV-2 Binding to Receptors on the Cell Surface (A) and Assay Set-up (B)

The Modular Octet® R Series

The Octet® R series utilize Bio-Layer Interferometry (BLI) label-free technology for multiple applications in biomolecular interactions analysis. They are available in configurations of 2, 4 and 8 channels (Figure 2) that can be field upgraded from lower to higher channels, thereby providing researchers with the flexibility to upgrade their current instrument according to their throughput needs and budget (Table 1).

Data described in this study were generated using the Octet® R4 BLI system; suitably designed for laboratories with mid-size throughput needs.

	Octet® R2 BLI System	Octet® R4 BLI System	Octet® R8 BLI System
Number of Spectrometers	2	4	8
Maximum Simultaneous Reads	2	4	8
Temperature Control	15–40 °C	15–40 °C	15–40 °C
Evaporation Control	No	No	Yes
GxP Package Availability	No	No	Yes

Table 1: Features and Specs of the Modular Octet® R Series



Figure 2: The Modular Octet® R Series; Similar Design, Different Read Heads. The Octet® R4 BLI System can be used to detect up to 4 samples in parallel.

Materials and Methods

Materials

Samples

- Biotinylated Human ACE2 / ACEH Protein (111.7 kDa), Fc, AviTag™ (ACRO Biosystems Cat. No. AC2-H82F9-25ug)
- SARS-CoV-2 (COVID-19) S protein RBD (26.5 kDa), His Tag (MALS verified) from ACRO Biosystems (Cat. No. SPD-C52H3-100ug)
- SARS-CoV-2 S protein (138 kDa), His Tag, Super stable trimer (MALS and NS-EM verified) from ACRO Biosystems (Cat. No. SPN-C52H9-50ug)

Instrument

- The modular Octet® R4 BLI system with Octet® BLI Discovery and Analysis Studio Software (v13) was used for the studies

Biosensors

- Streptavidin (SA: Cat. No. 18-5019)

Sample plates

- 96-well, black, flat bottom microplate, Greiner Bio-One Cat. No. 655209

Assay Buffers

- PBS, pH 7.4 with 0.002% P20 and 0.1% BSA

Methods

Assay optimization was first performed to establish suitable buffer and optimal ligand loading conditions. Biotinylated ACE2 protein was immobilized to Streptavidin (SA) biosensors at concentrations ranging from 0.75 µg/mL (6.71 nM)–3 µg/mL (26.86 nM) to achieve a loaded surface density ranging from 0.6nm–about 1.0 nm respectively. The S1 trimer was presented as analyte at concentrations ranging from 100, 50, 12.5, 6.25, 1.563, 0.7813 and 0 nM to determine its binding kinetics to the immobilized ACE2. The binding kinetics of RBD variants (wild type and Delta) to ACE2 was determined at RBD (analyte) concentrations ranging from 150, 75, 37.5, 18.75, 9.375, 4.688, 2.34 and 0 nM.

Prior to the start of the assay, the SA biosensors were hydrated (pre-wet) for at least 10 minutes in the assay buffer. The assay design varied based on the interaction studied, but typically included the following assay steps:

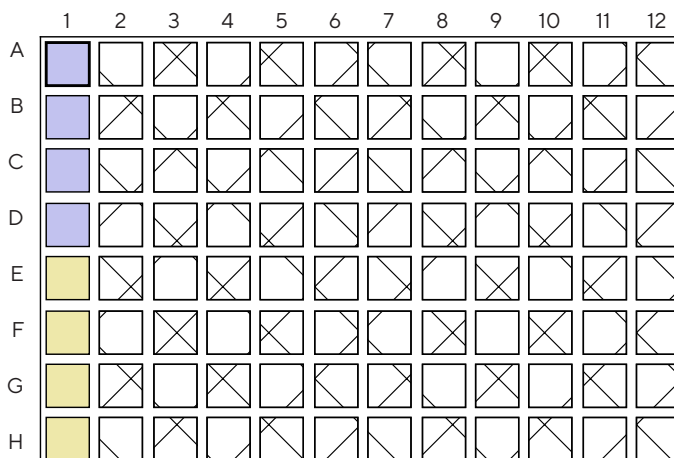
- The hydrated biosensors were dipped in assay buffer for 30 seconds to establish an initial baseline (biosensors equilibration)
- The biosensors were then dipped in the biotinylated ligand for 240–600 seconds (ligand load step), followed by assay buffer for 60 seconds (baseline 2)

- The ligand-bound biosensors were dipped for 90–450 seconds in different concentrations of the analyte sample (association step) and for 180–600 seconds in assay buffer (final, dissociation step).

Appropriate controls for non-specific binding of analyte (reference sensor with no ACE2 immobilized) and buffer blank (reference well with zero analyte concentration) were included in the assays. To measure the thermodynamics of the interactions, the binding kinetics was measured at assay temperature varying from 15 °C, 20 °C, 25 °C, 30 °C and 37 °C.

The kinetics data were analyzed using the Octet® Analysis Studio Software v13.0. The data were y-aligned to the last 5 s of baseline, inter-step corrected to dissociation and Savitsky Golay filtering applied. Data were fitted with a 1:1 model with Global fit settings.

Biosensor Tray Layout



Sample Plate Layout

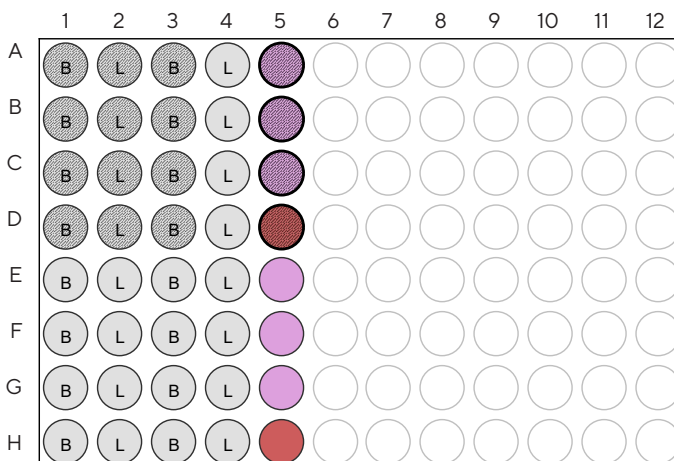


Figure 3: Octet® R4 Protein-Protein Binding Kinetics Method Showing Biosensor and Sample Trays Setup With 4 Biosensors Used in Tandem for 3 Concentration Points Plus Reference Well. This design can be used for 1 run, 2 assays and 1 replicate. A second run with a second column of biosensors would be needed to achieve 2 replicates.

Assay Setup

The Octet® R4 BLI system can be used to perform up to 4 measurements in parallel (Figure 3). For these studies (kinetics dose response analysis with 6 or 7 concentration points), the assay was performed in 2 runs with the first 4 biosensors (blue) dipping into the

top 3 concentrations plus a buffer-only reference while the second 4 biosensors (yellow) were dipped into the bottom 3 concentrations plus a buffer-only reference. The data were later merged and analyzed in the Octet® Analysis Studio Software.

Transition and Equilibrium State Thermodynamics Calculations:

The changes in the transition state and equilibrium state thermodynamic parameters of enthalpy (ΔH), entropy (ΔS) and Gibbs free energy (ΔG) was calculated using Eyring and Van 't Hoff's equations respectively.

Eyring equation $K^\ddagger = kh/k_B T$ was rearranged and derived for transition state thermodynamics to give:

$$\ln(kh/k_B T) = -\Delta H^\ddagger/RT + \Delta S^\ddagger/R \quad (\text{Equation 1})$$

Similarly, Van 't Hoff's equation $\Delta G^\circ = -RT \ln K_D$ in conjunction with the relationships

$$\Delta G^\circ = \Delta H^\circ - T\Delta S^\circ$$

was rearranged to give:

$$\ln K_D = \Delta H^\circ/RT - \Delta S^\circ/RT \quad (\text{Equation 2})$$

K^\ddagger = Equilibrium constant for the formation of transition state

k = kinetic rate constant for each corresponding reaction; k_a = forward reaction and k_d = reverse reaction

k_B = Boltzman's constant

h = Planck's constant

ΔG° and ΔG^\ddagger = Change in Equilibrium and transition state free energies respectively

ΔH° and ΔH^\ddagger = Change in equilibrium and transition state enthalpy respectively

ΔS° and ΔS^\ddagger = Change in equilibrium and transition state entropy respectively

T = Temperature (K)

Results and Discussions

Effect of Conformation in the Binding of SARS-CoV-2 to ACE2 Protein

It has been suggested that SARS-CoV-2 virus appears to be optimized for binding to the human receptor ACE2 and that similarity exists between ACE2's binding to both CoV-2 and CoV-1 at the receptor binding domain (RBD). It is also noted that the trimeric spike glycoprotein of SARS-CoV-2 is comprised of three S1/S2 units, and that the RBD is contained within the S1 subunit. Conformational changes at the S1/S2 units play a critical role in the binding behavior of ACE2 to the RBD. In this application note, a side-by-side comparison of the binding of the ACE2 protein (immobilized on a streptavidin biosensor) binding to the RBD and the trimeric protein reveals that the ACE2 binds with

> 15-fold higher affinity to the trimer than to RBD (Figure 4, Table 2). The kinetics rate data further suggest that while the binding site on the RBD is more readily accessible to the ACE2 than in the trimer, once bound, dissociation is slower in the trimer suggesting that structure plays a key role in the binding and by extension the subsequent biological activity of SARS-CoV-2. In line with this, it has been previously suggested that⁵ after binding to the receptor, the following cascade of events is triggered: the spike protein undergoes a large conformational change, the S1 with the receptor is shed, the S2 interaction conformationally shifts to a more stable post-fusion state, and finally the viral membrane is fused with the cell.

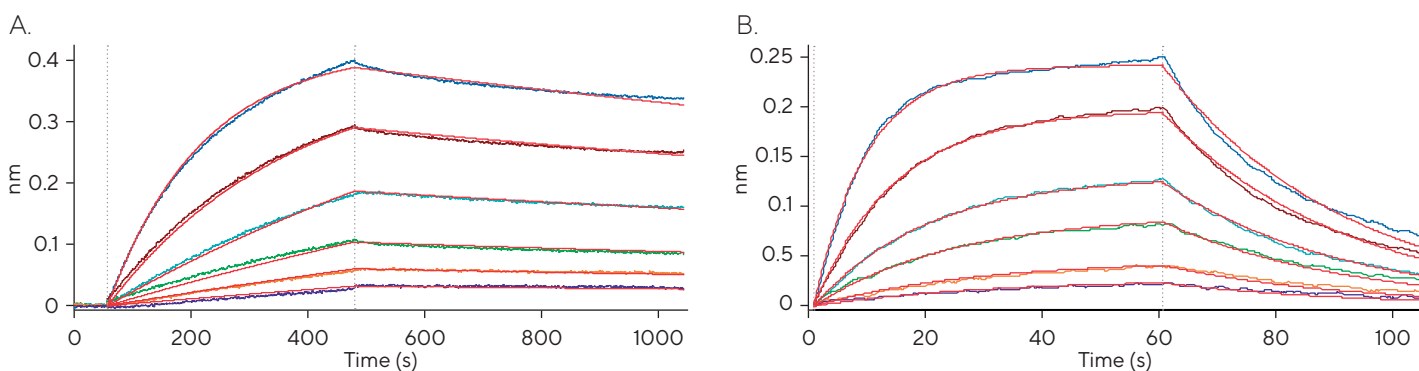


Figure 4: SARS-CoV-2 Spike Trimer (A) and RBD (B) Binding to ACE2 Protein Immobilized on the Biosensor Surface

Binding Mode	k_a ($M^{-1}s^{-1}$)	k_d (s^{-1})	K_D (nM)
RBS	$(4.5 \pm 0.8) \times 10^5$	$(3.3 \pm 0.1) \times 10^{-2}$	76 ± 15
Trimer	$(5.9 \pm 0.4) \times 10^4$	$(2.76 \pm 0.01) \times 10^{-4}$	4.7 ± 0.3

Table 2: Binding Parameters for Spike RBD and Trimeric Binding Protein Binding to ACE2. Biotinylated ACE2 was immobilized onto high precision streptavidin biosensors.

Thermodynamics of Equilibrium of Binding of SARS-CoV-2 RBD to ACE2 Protein

Binding kinetics data can be used to estimate thermodynamic binding parameters for the interaction of biological molecules and to evaluate binding stability. The equilibrium constant for the formation of the transition-state of a reaction can be related to the rate constant of the overall reaction using the Eyring equation (Equation 1). A rearrangement of the thermodynamic equations for the transition state can be used to obtain the thermodynamic transition state constants for the forward and reverse reactions by plotting $\ln(k_a/T)$ and $\ln(k_d/T)$ against $1/T$ respectively.

To enable thermodynamics analysis of ACE2 binding to SARS-CoV-2 binding domains, temperature-dependent binding analyses were performed on the Octet[®] R4 BLI system at five different sample plate temperature conditions: 15 °C, 20 °C, 25 °C, 30 °C and 37 °C respectively (Figure 5, Table 3).

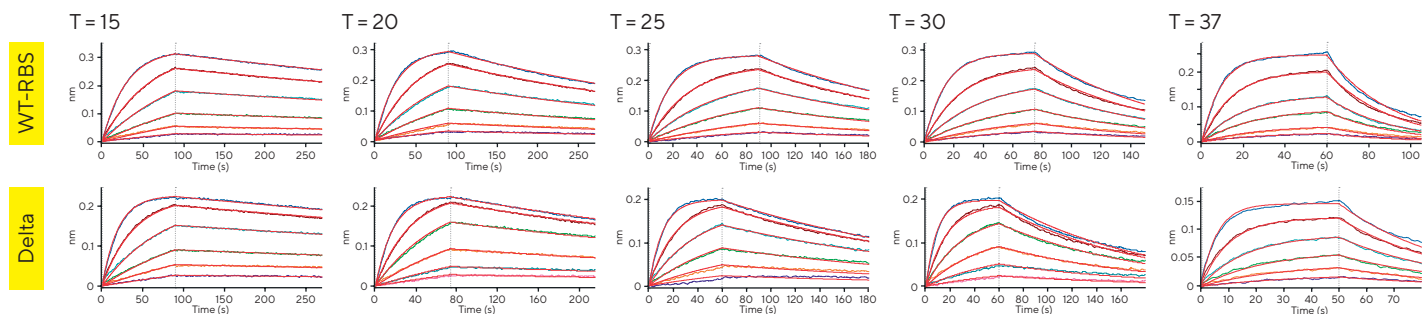


Figure 5: Temperature Dependent Binding Curves of SARS-CoV-2 WT- and Delta-Variants of RBDs Binding to ACE2

Temperature (°C)	WT-RBD			Delta-RBD		
	k_a (M ⁻¹ s ⁻¹)	k_d (s ⁻¹)	K_D (nM)	k_a (M ⁻¹ s ⁻¹)	k_d (s ⁻¹)	K_D (nM)
15	$(2.10 \pm 0.02) \times 10^5$	$(1.15 \pm 0.02) \times 10^{-3}$	5.50 ± 0.01	$(3.0 \pm 0.3) \times 10^5$	$(8.6 \pm 0.5) \times 10^{-4}$	2.8 ± 0.2
20	$(2.6 \pm 0.1) \times 10^5$	$(2.45 \pm 0.01) \times 10^{-3}$	9.7 ± 0.3	$(3.77 \pm 0.04) \times 10^5$	$(2.02 \pm 0.08) \times 10^{-3}$	5.3 ± 0.1
25	$(3.3 \pm 0.1) \times 10^5$	$(5.8 \pm 0.2) \times 10^{-3}$	17 ± 1	$(5.5 \pm 0.1) \times 10^5$	$(4.70 \pm 0.04) \times 10^{-3}$	8.60 ± 0.06
30	$(3.7 \pm 0.1) \times 10^5$	$(1.2 \pm 0.4) \times 10^{-3}$	32.8 ± 0.2	$(6.4 \pm 0.5) \times 10^5$	$(1.0 \pm 0.2) \times 10^{-2}$	16 ± 4
37	$(4.5 \pm 0.8) \times 10^5$	$(3.3 \pm 0.1) \times 10^{-2}$	76 ± 15	$(1.0 \pm 0.2) \times 10^6$	$(2.5 \pm 0.1) \times 10^{-2}$	24 ± 3

Table 3: Binding Parameters for SARS-CoV-2 Wild Type and Delta-Mutant RBDs Binding to ACE2

As temperature increases, both the association rate constants and the dissociation rate constants increase for both wild type and Delta RBD domains (Figure 6). Equilibrium dissociation constants (K_D) also increase

suggesting a weaker interaction with increasing temperature largely driven by faster dissociation for both molecules.

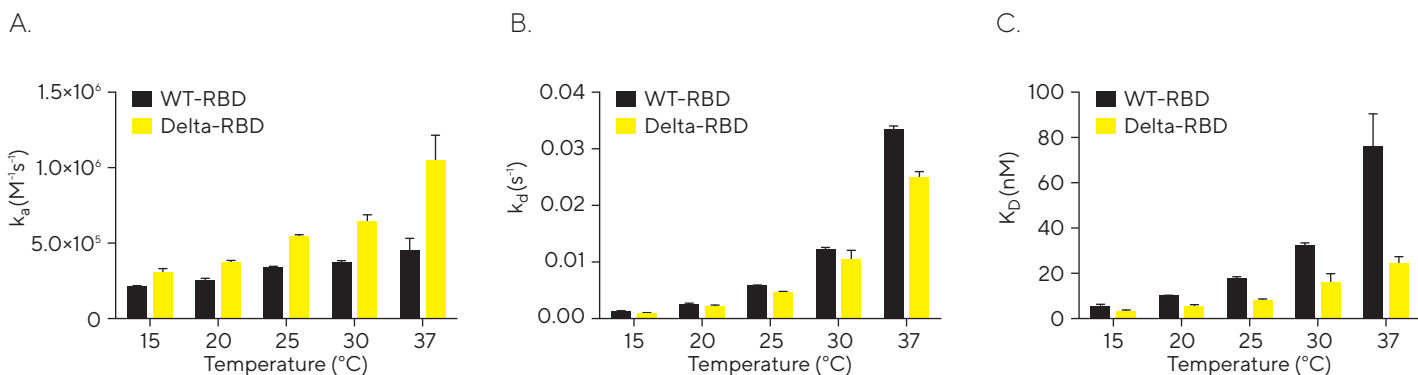


Figure 6: Temperature Dependence of Kinetics (A) On-Rates, (B) Off-Rates, and (C) Affinities of SARS-Cov-2 WT- And Delta-Variant RBDs Binding to ACE2

The temperature-dependent affinities of interaction can be used to calculate entropies and enthalpies of the interactions using the Van 't Hoff equation. In addition, the measured rates of association and dissociation respectively as a function of temperature can be used to calculate the interactions transition-state enthalpy and entropy using the Eyring equation. Eyring plots for association, dissociation rate constants and for equilibrium dissociation constants are shown in Figure 7. The Eyring plots can be used to extract values for $\Delta H^\ddagger/R$ (slope of the linear plot),

and ΔS^\ddagger (y-intercept of the linear plot) from which ΔG^\ddagger (free energy) values can be calculated for both association and dissociation transition-state. Similarly, a rearranged Van 't Hoff's equation (Equation 2) can be used to calculate thermodynamics parameters for the equilibrium states of binding. Understanding the transition-state formation mechanism allows for a further understanding on why interactions with similar affinities can exhibit different kinetics.⁶

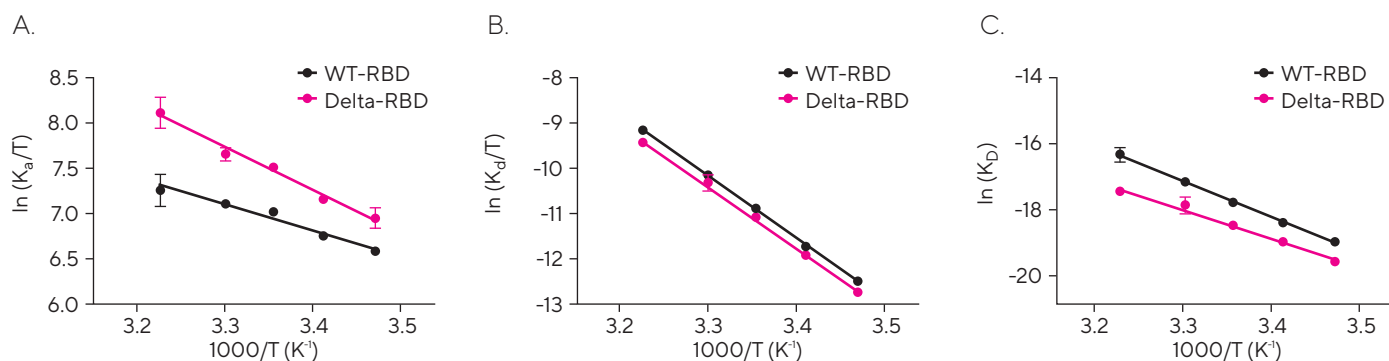


Figure 7: Effect of Temperature on the Rates of Binding (A) On-Rates, (B) Off-Rates and (C) Affinity Constants of SARS-CoV-2 WT- and Delta-Variant RBDs Binding to ACE2

Transition-state and equilibrium-state energetics data for the binding of WT-RBD and Delta-RBD to ACE2 protein are shown in Tables 4 and 5.

Transition State Energetics						
Binding System	WT-RBD binding to ACE2			Delta-RBD binding to ACE2		
	ΔH^\ddagger (kJ/mol)	ΔS^\ddagger (J/mol · K)	ΔG^\ddagger (kJ/mol)	ΔH^\ddagger (kJ/mol)	ΔS^\ddagger (J/mol · K)	ΔG^\ddagger (kJ/mol)
Association	23.2	-77.0	46.2	38.5	-21.4	44.9
Dissociation	112.5	74.4	90.3	111.7	69.8	90.3

Table 4: Transition State Binding Energetics for SARS-CoV-2 Wild Type and Delta-Mutant RBDs Binding to ACE2

Equilibrium State Energetics					
WT-RBD binding to ACE2			Delta-RBD binding to ACE2		
ΔH° (kJ/mol)	ΔS° (J/mol · K)	ΔG° (kJ/mol)	ΔH° (kJ/mol)	ΔS° (J/mol · K)	ΔG° (kJ/mol)
-89.2	-151.1	-44.1	-73.2	-91.4	-46.0

Table 5: Equilibrium-State Binding Energetics for SARS-CoV-2 Wild Type and Delta-Mutant RBDs Binding to ACE2

Transition-state energetics provide insights into the barriers the ligand needs to overcome to attain a final stable state. Whereas the enthalpic energies may be linked to polar interactions between the interacting partners,⁶ the entropic energies are linked to the flexibility of the interaction and potential solvation effects.

In this study, the energetics data show minimal differences in the transition-state for both association and dissociation between the wild type and the Delta mutant. A further examination of the transition-state energetics reveals that any differences observed are largely driven by the

association transition-state formation. The data suggest a higher enthalpic energy barrier for the interaction between the Delta-RBD and the ACE2 protein than for the wild type. There is however a significant difference in the entropic values for both transition-state formation and the final equilibrium state suggesting that the molecular disorder during binding plays a key role. The wild type RBD exhibits lower entropy than the Delta variant suggesting a more favorable binding event with the Delta variant than the wild type RBD.

Conclusion

In this short application note, the modular Octet® R4 BLI system has been used to showcase a simple method that deploys binding kinetics parameters at varying temperatures and utilizes the Eyring and Van 't Hoff equations to derive binding thermodynamic parameters. Such parameters can help explain the barriers ligands need to overcome to achieve a stable complex upon binding. When coupled with structural knowledge of the binding partners, the data can further provide insights into the effect of structural differences in the binding mechanisms and by extension the effect of mutations such as with the different variants of SARS-CoV-2 in the rates of binding or infectivity.

The modular Octet® BLI systems are available in three different configurations of 2, 4 and 8 channels respectively. They provide researchers with options based on throughput needs and budgetary constraints while achieving similar high-quality data results. The lower channel Octet® R systems (R2 and R4) are field upgradable to the higher channel system (R8) allowing for future instrument upgrades.

References


1. Yan R, Zhang Y, Li Y, Xia L, Guo Y, Zhou Q. Structural basis for the recognition of SARS-CoV-2 by full-length human ACE2. *Science*. 2020;367(6485):1444-1448. doi:10.1126/science.abb2762
2. Stancioiu F, Papadakis GZ, Kteniadakis S, et al. A dissection of SARS CoV2 with clinical implications (Review). *Int J Mol Med*. 2020;46(2):489-508. doi:10.3892/ijmm.2020.4636
3. Sharifkashani S, Bafrani MA, Khaboushan AS, et al. Angiotensin-converting enzyme 2 (ACE2) receptor and SARS-CoV-2: Potential therapeutic targeting. *Eur J Pharmacol*. 2020;884:173455. doi:10.1016/j.ejphar.2020.173455
4. Wrapp D, Wang N, Corbett KS, et al. Cryo-EM structure of the 2019-nCoV spike in the prefusion conformation. *Science*. 2020;367(6483):1260-1263. doi:10.1126/science.abb2507
5. Anand SP, Chen Y, Prévost J, et al. Interaction of Human ACE2 to Membrane-Bound SARS-CoV-1 and SARS-CoV-2 S Glycoproteins. *Viruses*. 2020;12(10):1104. Published 2020 Sep 29. doi:10.3390/v12101104
6. Deganutti G, Zhukov A, Deflorian F, et al. Impact of protein-ligand solvation and desolvation on transition state thermodynamic properties of adenosine A2A ligand binding kinetics. *In Silico Pharmacol*. 2017;5(1):16. Published 2017 Nov 20. doi:10.1007/s40203-017-0037-x

Germany

Sartorius Lab Instruments
GmbH & Co. KG
Otto-Brenner-Strasse 20
37079 Goettingen
Phone +49 551 308 0

USA

Sartorius Corporation
565 Johnson Avenue
Bohemia, NY 11716
Phone +1 888 OCTET 75
Or +1 650 322 1360

 For additional information,
visit www.sartorius.com